On the Feasibility of Non-contact Cardiac Motion Sensing for Emerging Heart-based Biometrics

Yan Zhuang[1], Chen Song[1], Feng Lin[1], Yiran Li[2], Changzhi Li[2], Wenyao Xu[1]

[1] Department of Computer Science and Engineering, SUNY at Buffalo, Buffalo, NY, USA
[2] Department of Electrical and Computer Engineering, Texas Tech University, Lubbock, TX, USA
Email: {yanzhuan, csong5, flin28, wenyaoxu}@buffalo.edu
{yiran.li, changzhi.li}@ttu.edu

***Abstract*— Cryptographic security is of great importance. Biometrics play a vital role in modern authentication systems. Among all emerging biometrics, heart-based biometrics are promising because they are unique and hard to counterfeit. The current solutions on cardiac motion detection are either obtrusive or incapable of providing comprehensive cardiac motion information. To this end, we present Non-contact Cardiac Motion Sensing (NCMS), an end-to-end hardware and software solution, to sense and characterize the cardiac motion in a continuous, unobtrusive and user-friendly manner. We evaluate the performance of NCMS and compare the cardiac motion cycle on human subjects. Experimental results indicate the feasibility of NCMS to detect the cardiac motion and show the concept of a new modality in emerging heart-based biometrics.**

***Index Terms*— Cardiac biometric, tiny signal detection and demodulation.**

I. Introduction

Cryptographic systems often rely on the secrecy of cryptographic credentials, which however, are vulnerable to eavesdropping (either via malware or shoulder surfing). To date, more than 60% of IT systems are under unauthorized access due to the weakness of cryptographic mechanism, which leads to serious financial and privacy loss.

Biometric-based authentication uses physiological and behavioral characteristics. Despite of their advantages, most of the biometric traits have certain drawbacks that can severely threaten the security. Some can be easily forged (e.g. face, typing dynamics). Some can be altered or imitated (e.g. gait, voice). Few others can be used even in the absence of the person (e.g. finger print). Iris/DNA are more secure ones yet introduce different usability challenges in the existing practice.

As an emerging biometric, heart-based biometrics are of great interest. The characters in cardiac motion are tightly coupled with multiple biological traits, including the heart structure, blood circulation system and other related tissues. These personal body features make the cardiac motion a unique identity for each individual [1]. Moreover, since it is intrinsically connected to multiple biological functions, the cardiac motion is extremely difficult to counterfeit or to hide for a living individual.

As a modern technology, Magnetic resonance imaging (MRI) [2] can provide detailed information of the cardiac motion. However, the potential radiation harm prevents MRI from daily use. To date, electrocardiography (ECG) is still the primary method to characterize the cardiac motion in clinical use. By attaching the electrodes on the patient's body, we can detect the electrical signal changes caused by the activity of both atria and ventricles during each heartbeat. Nevertheless, this method suffers from several drawbacks including invasiveness and attended installation.

Recent research is seeking for the non-contact and cost-effective cardiac motion detection on approaches. Lubecke *et al.* [3] and Huang *et al.* [4] used an electromagnetic sensor to detect the heartbeat rhythm information via vital signs. However, they were not able to further obtain the comprehensive cardiac motion information with ample medical and health information.

In this work, we present Non-contact Cardiac Motion Sensing (NCMS), which is the first attempt to characterize the cardiac motion in a non-contact manner. Specifically, 1) we design and implement an electromagnetic probe (EM-probe) based on the commercial off-the-shelf (COTS) components, which is able to accurately detect the cardiac motion; 2) we evaluate the performance of NCMS and compare the obtained cardiac features within the cardiac motion cycles from human subjects.

II. Mechanism of Cardiac Motion

Cardiac motion is the 3-D automatic heart deformation caused by the self excitement of cardiac muscle. It is coordinated by the sinoatrial (S-A) and atrioventricular (A-V) nodes. The human heart contains four cavities. The two upper cavities are atria and the two bottom chambers are ventricles (Fig. 1(a)). The successive contraction and relaxation of both atria and ventricles circulate the oxygen-rich blood throughout the body, which form the cardiac motion. The contraction is called systole and the relaxation is called diastole. In one cardiac cycle, ventricles relax and passively fill with approximate 70% of their total volume.

978-1-4673-9806-0/16/$31.00 © 2016 IEEE

Then atria expands to extract and pump blood. Meanwhile, ventricles continuously fill with the remaining 20% (ventricles always free 10% of the volume for contraction). After that, ventricles start to contract with heart muscles, and the blood volume keeps uncharged. When inside pressure reaches a contain threshold between ventricles and atria, blood is ejected and the heart volume reduces rapidly [5]. As discussed above, one cardiac motion cycle consists of five distinct stages in atria and ventricles, including 1) ventricular filling (VF), 2) atrial systole (AS), 3) isovolumetric ventricular contraction (IC), 4) ventricular ejection (VE) and 5) isovolumetric ventricular relaxation (IR) [5] (Fig. 1(b)). These stages are significantly different among people in volume, surface shape, moving dynamics (e.g. speed and acceleration) and 3-D deformation of heart.

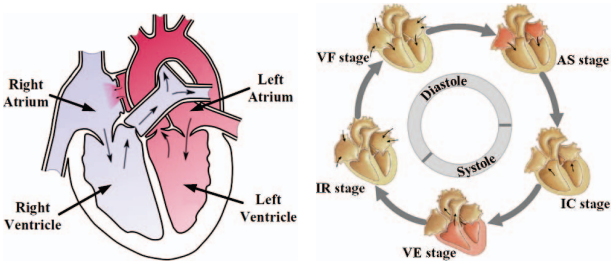

(a) The structure of the heart. (b) The five cardiac motion stages.

Fig. 1. Mechanism of cardiac motion.

III. Electromagnetic Probe (EM-probe) and Baseband Signal Demodulation

NCMS is accomplished in a non-contact way based on EM-probe. It generates a single-tone carrier signal towards the subject. When the microwave hits the subject, the body displacement (caused by the heartbeat) of the subject introduces a phase shift. By demodulating this phase information, we can obtain the cardiac motion information.

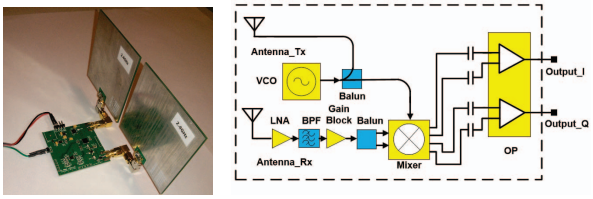

(a) EM-probe. (b) The block diagram of EM-probe.

Fig. 2. The block diagram of EM-probe, which captures the heartbeat-related signal and outputs the baseband signal.

Fig. 2 depicts the function block diagram of EM-probe. It adopts direct-conversion radar architecture to capture the cardiac motion signal (Fig. 2(b)). Specifically, the voltage controlled oscillator (VCO) in the transmitter generates a 2.4 GHz carrier signal, which provides local oscillator (LO) to the mixer in the receiver chain. The output power of this transmitter is around 0 dBm. The receiver chain consists of a low noise amplifier (LNA), a band pass filter (BPF), a gain block, a balun, a mixer, and two baseband operational amplifiers (OPs). The function of LNA is to amplify the received signal at 2.4GHz. The BPF filters the interference signals with frequencies outside the 2.4 GHz. A gain block is ultilized to further amplify the received signal. Then, the down-converted $I(t)$ and $Q(t)$ baseband signals are amplified using two OPs with the same gain of 40 dB [6]. Finally, NI USB-6008 (an NI data acquisition devices (DAQ)) digitizes the baseband in-phase $I(t)$ and quadrature $Q(t)$ signal. For simplicity, our work describes the $I(t)$ and $Q(t)$ as in Eq. (1):

$$\begin{cases} I(n) = A_0 cos(\frac{4\pi x(n)}{\lambda}) + DC_I \\ Q(n) = A_0 sin(\frac{4\pi x(n)}{\lambda}) + DC_Q \end{cases}. \quad (1)$$

According to the trigonometric identities, the samples of *I/Q* channels stay on a circle whose center is (DC_I, DC_Q) with a radius of A_0. Given $I(t)$ and $Q(t)$, we identify the three unknown parameters: DC_I, DC_Q, and A_0 using the least square optimization method. Then, we employ an extended differentiate and cross multiple (DACM) algorithm proposed by Wang *et al.* [7] to obtain the displacement signal $x(t)$. This extended DACM algorithm, as described in Eq. (2), avoids the discontinuity problem and is robust to the random noise.

$$\Phi[n] = \sum_{k=2}^{n} \frac{I[k]\{Q[k] - Q[k-1]\} - \{I[k] - I[k-1]\}Q[k]}{I[k]^2 + Q[k]^2}. \quad (2)$$

IV. Evaluation

Fig. 3 depicts the experimental setup. The subject sits in a chair in a relaxed condition while the EM-probe is placed 20cm in front of him. When EM-probe starts to detect the cardiac motion, the subject begins to breath normally and an e-health platform [8] simultaneously collects the ECG signal as the ground truth signal via attached electrodes. Both the EM-probe and ECG signal are synchronized and sampled at 100Hz using a NI USB-6008 DAQ device.

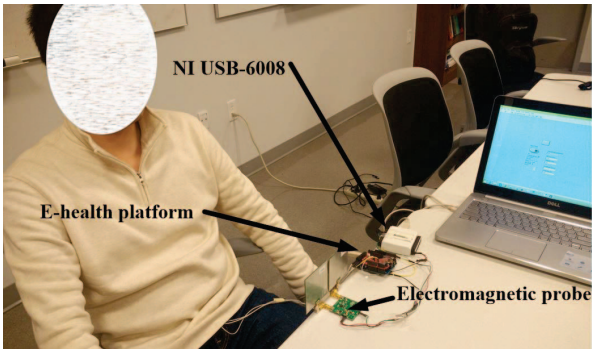

Fig. 3. The demonstration of the experimental setup.

The detected cardiac motion is a periodical heart movement signal. We first segment the periodical signal sequence into the discrete cardiac motion cycles. As shown

in Fig. 4(a), each segment is further split into five sub-frames according to the cardiac motion cycle (see Sec. II).

Fiducial points are the points contain the unique and non-volatile biological information in individuals. The fiducial points we select are VFP, ICP, VEP and IRP, which are defined as follows:

- VFP is a local maximum point in the segment, which indicates the onset of atrial systole period where the atrial muscles contract to squeeze the blood into the ventricles.
- ICP is a local maximum point in the segment, which locates at the end of isovolumetric ventricular contraction stage and implies the beginning of ventricular ejection stage.
- VEP is a specific local minimum point that represents the end of ventricular ejection period.
- IRP is a local minimum point that stands for the end of isovolumetric ventricular relaxation stage, the final stage of the cardiac motion cycle.

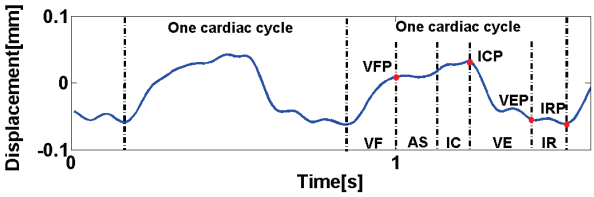

(a) The detected signal with the fiducial points in a cardiac cycle.

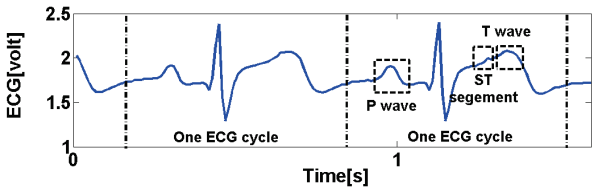

(b) The ECG signal serves as the ground truth signal.

Fig. 4. The obtained cardiac motion signal and corresponding ECG ground truth signal.

The corresponding ECG signal is employed as the ground truth (Fig. 4(b)). We can observe that the cardiac motion cycles in the sampled signal match the ECG ground truth signal precisely. Our selected fiducial points in the cardiac motion cycle agree with those in the ECG waveform, which contain the same physical meaning. Specifically, VFP, which indicates the beginning of atrial systole stage, is aligned with the P segment in the ECG waveform, which represents the atrium squeeze. ICP and VEP are at the onset and end of ventricular ejection stage, which corresponds with the ST segment and T segment. IRP is in the end of a segment, whose location also agrees with the end of the ECG waveform cycle. Therefore, the ECG ground truth waveform verifies our sampled data and selected fiducial points.

We also compare the data from two subjects. As shown in Fig. 5, the duration of the cardiac cycle of Subject 1 is much longer than that of Subject 2, implying a slower heart rate of Subject 1. The difference in amplitude indicates that the heart of Subject 2 contracts more volume than that of Subject 1. The shape of displacement for both two subjects varies, indicating that the different cardiac dynamics such as the speed and acceleration of contraction and relaxation of the cardiac muscle vary during different cardiac motion stages. Moreover, the duration of VF and IC of Subject 1 (the segment between VFP and ICP) is longer than that of Subject 2, while the duration of IC and VE of Subject 1 (the segment between ICP and VEP) is shorter.

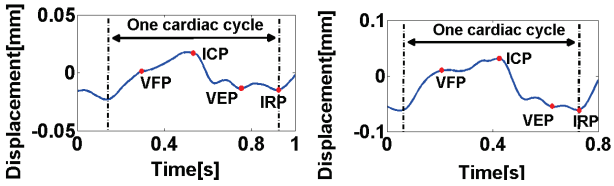

(a) The cardiac motion of Subj. 1. (b) The cardiac motion of Subj. 2.

Fig. 5. The comparison of cardiac motions from two subjects.

V. Conclusion

An end-to-end hardware and software solution NCMS has been represented to detect and characterize the cardiac motion features in a non-contact, continuous and user-friendly manner. We define the fiducial points and verify the correctness of NCMS. We compare the significant distinctions of the data from different subjects and prove the feasibility of NCMS for emerging heart-based biometrics.

Acknowledgment

This work is in part supported by NSF ECCS-1254838, CNS-1423061, ECCS-1462498 and CNS-1547167.

References

[1] Z. Zhang, H. Wang, A. V. Vasilakos, and H. Fang, "ECG-cryptography and authentication in body area networks," *IEEE Transactions on Information Technology in Biomedicine*, vol. 16, no. 6, pp. 1070–1078, 2012.

[2] W. Hollingworth, C. J. Todd, M. I. Bell, Q. Arafat, S. Girling, K. R. Karia, and A. K. Dixon, "The diagnostic and therapeutic impact of MRI: an observational multi-centre study," *Clinical radiology*, vol. 55, no. 11, pp. 825–831, 2000.

[3] O. B. Lubecke, P.-W. Ong, and V. Lubecke, "10 GHz doppler radar sensing of respiration and heart movement," in *Proceedings of the IEEE 28th Annual Northeast Bioengineering Conference*. IEEE, 2002, pp. 55–56.

[4] M.-C. Huang, J. Liu, W. Xu, C. Gu, C. Li, and M. Sarrafzadeh, "A self-calibrating radar system design for measuring vital signs," *To appear IEEE Transactions on Biomedical Circuits and Systems*.

[5] K. E. Barrett, S. M. Barman, S. Boitano, and H. Brooks, *Ganong's review of medical physiology*. New Delhi: McGraw Hill, 2010.

[6] Y. Li, C. Gu, T. Nikoubin, and C. Li, "Wireless radar devices for smart human-computer interaction," in *IEEE 57th International Midwest Symposium on Circuits and Systems (MWSCAS)*. IEEE, 2014.

[7] J. Wang, X. Wang, L. Chen, J. Huangfu, C. Li, and L. Ran, "Noncontact distance and amplitude-independent vibration measurement based on an extended dacm algorithm," *IEEE Transactions on Instrumentation and Measurement*, vol. 63, no. 1, pp. 145–153, 2014.

[8] *e-Health Sensor Platform V2.0*, Cooking Hacks, 2013.